Biosensors

DOI: 10.1002/anie.201008204

Quantitative 3D Analysis of Nitric Oxide Diffusion in a 3D Artery Model Using Sensor Particles**

*Michya Matsusaki, Suzuka Amemori, Koji Kadowaki, and Mitsuru Akashi**

A blood vessel is crucial not only for circulatory diseases and treatments, but also for the biological evaluation of drug diffusion to target tissues, the penetration of cancer cells or pathogens, and the control of blood pressure. A blood vessel is generally composed of three distinct layers: the intima, an inner single layer of endothelial cells (ECs); the media, medium layers of smooth muscle cells (SMCs); and the adventitia, an outer layer of fibroblast cells.[1] The ECs act as a sensing surface to transduce hydrodynamic forces and chemical stimuli into extracellular signal molecules such as endothelin-1, prostacyclin, and nitric oxide, which affect vascular events such as the contraction and relaxation of SMCs.[2] Nitric oxide (NO), produced by the nitric oxide synthase (NOS) protein family, is a lipophilic, highly diffusible, and short-lived physiological messenger.[3] It is well known that NO regulates a variety of important physiological responses including vasodilation, respiration, cell migration, and apoptosis.[4] The NO produced from ECs diffuses into SMCs through their cell membranes, and activates guanylate cyclase to produce intracellular cyclic guanosine monophosphate (cGMP), which induces a signaling pathway mediated by kinase proteins leading to SMC relaxation.[5a] Accordingly, quantitative, kinetic, and spatial analyses of the extracellular delivery of NO molecules from the EC layer to the SMC layers upon drug stimulation are crucial for pharmaceutical and biomedical evaluations of hypertension and diabetes. So far, pharmaceutical assays of NO production have been performed by in vivo animal experiments, but low reproducibility and difference of NO production depending on animal types are unsolved issues. Malinski and co-workers reported the in situ analysis of NO diffusion using the extracted animal aorta, but special equipment and techniques were necessary for their analysis method.[5b,c] Thus, the development of a convenient and versatile method for the in vitro quantitative and spatial analyses of NO diffusion inside the artery wall instead of animal experiments is important for biological and pharmaceutical applications.

In a previous study, we reported biocompatible and highly sensitive NO sensor particles prepared by layer-by-layer (LbL) assembly. The mesoporous, micrometer-sized silica particles encapsulating 4,5-diaminofluorescein (DAF-2), NO fluorescent indicator dye,[6] were covered with biocompatible chitosan (CT)–dextran sulfate (DS) LbL films to provide cytocompatibility and to inhibit leakage of DAF-2. The NO sensor particles (SPs) showed high NO sensitivity at 5–500 nM, which is sufficient to detect NO at concentrations of hundreds of nM (EC production level[7a]).[7b] If an artificial three-dimensional (3D) artery model allocating these SPs can be developed, the extracellular diffusion of NO from the EC layer to the SMC layers with chemical and physical stimuli is expected to be observed in vitro fluorescently by using confocal laser scanning microscopy (CLSM).

Herein, we demonstrate for the first time spatial and quantitative analyses of NO diffusion from the EC layer to the SMC layers using a 3D artery model with SPs allocated into each cellular layer (Figure 1). Recently, we reported an in vitro hierarchical cell manipulation technique to develop 3D cellular multilayers by the fabrication of nanometer-sized extracellular matrix (ECM) films on the surface of each cell layer.[8] Approximately 6 nm thick fibronectin (FN)–gelatin (G) LbL films prepared on the surface of the first layer of cells can provide a suitable cell-adhesive surface that is similar to the natural ECM for the second layer of cells.[8a] Furthermore, 3D blood vessel models consisting of human ECs and SMCs were successfully developed, and their morphology and histology were evaluated in detail.[8d] Herein, we developed five-layered (5L) artery models including SPs using human aortic smooth muscle cells (AoSMCs) and human aortic endothelial cells (HAECs). The 3D structural effect of HAECs and AoSMCs on NO production from the HAECs was clarified in relation to the direction of interaction between these cells. Furthermore, a graded concentration change of NO from the uppermost HAEC layer to the underlying AoSMC layers was elucidated by 3D analysis using confocal laser scanning microscopy.

The SPs were prepared based on our previous report.[7b] The encapsulated DAF-2 in the mesoporous silica particles was stable even after 1 month of incubation in buffer (see Figure S1 in the Supporting Information) or 1 week of incubation in culture medium containing serum (data not shown). Since DAF-2 has a weak negative charge under neutral pH conditions, the electrostatic interaction with CT is

[*] Dr. M. Matsusaki, S. Amemori, K. Kadowaki, Prof. M. Akashi
Department of Applied Chemistry
Graduate School of Engineering, Osaka University
Yamada-oka, Suita, Osaka 565-0871 (Japan)
E-mail: akashi@chem.eng.osaka-u.ac.jp
Homepage: http://www.chem.eng.osaka-u.ac.jp/~akashi-lab/
Dr. M. Matsusaki
Precursory Research for Embryonic Science and Technology (PRESTO)
Science and Technology Agency (JST) (Japan)

[**] We thank Dr. M. Kino-oka and Dr. M.-H. Kim at Osaka University for CLSM observation. This work was supported mainly by PRESTO-JST, partly by an Industrial Technology Research Grant Program in 2006 (06B44017a) from NEDO of Japan, a Grant-in-Aid for Scientific Research on Innovative Areas (21106514) from MEXT of Japan, and by the Noguchi Institute.

Supporting information for this article is available on the WWW under http://dx.doi.org/10.1002/anie.201008204.

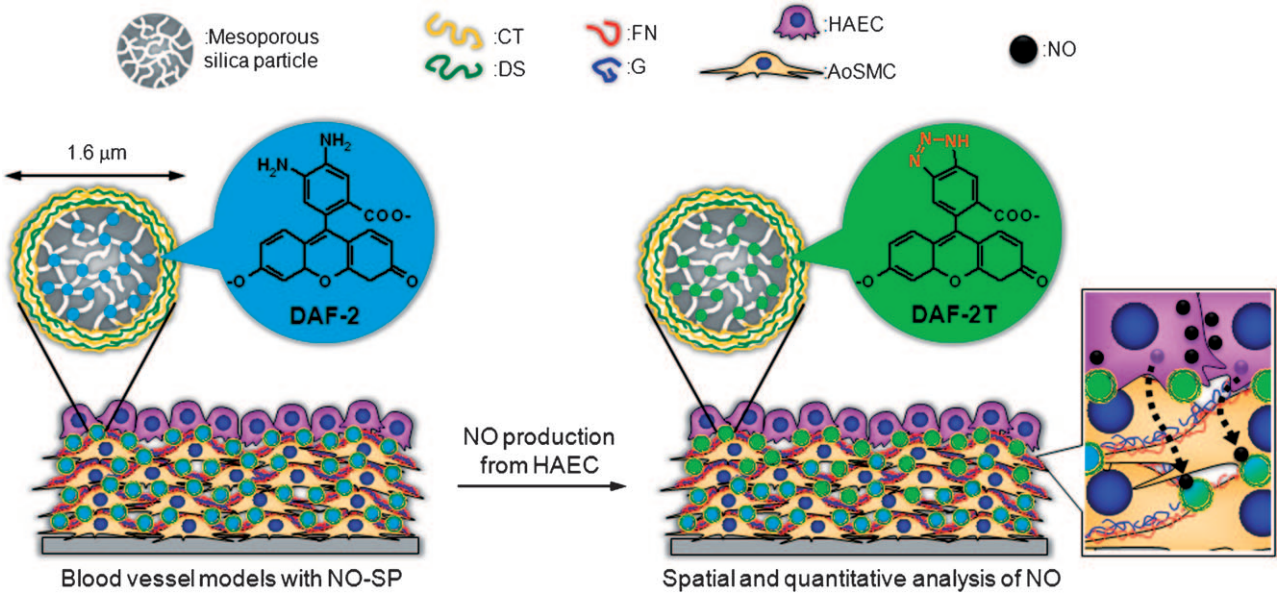

Figure 1. Schematic illustration of the in vitro spatial and quantitative analyses of NO diffusion from the uppermost EC layer to the SMC layers in a 3D artery model by SPs, which were allocated into each layer.

probably one of the reasons for this high stability. These micrometer-sized SPs (1.6 μm diameter) can avoid endocytosis and provide high biocompatibility and stable adsorption on the cell surface.[7b]

To clarify the effect of the layered structure consisting of AoSMCs and HAECs on NO production, the NO concentrations from various 2D or 3D structures consisting of AoSMCs and HAECs after 48 h of culture were evaluated by a horseradish peroxidase (HRP) assay[9a] (see Figures S2 and S3 in the Supporting Information). Figure S3 shows the NO concentrations of monolayered AoSMCs or HAECs (1L-AoSMC or 1L-HAEC), monolayered co-culture of both cells (1L-co-culture), and a bilayer of AoSMCs and HAECs after 48 h of culture. The NO production of the 1L-HAECs was fourfold higher than that of the 1L-AoSMCs, because the SMCs barely release any NO into the extracellular environment.[6a] Interestingly, the bilayer structure of HAECs with AoSMCs promoted twofold higher NO production relative to 1L-HAECs, whereas the heterogeneous monolayered co-culture with AoSMCs did not show any effect. The reason for this phenomenon is probably related to the direction of interaction between the HAECs and AoSMCs. A vertical interaction between upper HAECs and lower AoSMCs like a native artery may effectively stimulate NO production, because the ECs are known to have high polarity.

By using SPs, the localized NO concentration around the HAECs could be analyzed quantitatively. It has been predicted that the NO concentration on the membrane surface may vary from submicro- or micromolar levels,[5b] but distinct differences in NO concentration at various membrane positions have not been elucidated yet. Accordingly, we tried to clarify the difference in NO concentration at the apical and basal membranes of 1L-HAECs after the addition of bradykinin, which is an NO agonist peptide hormone, using SPs. Figure 2a,b show scanning electron microscopy (SEM) images of SPs on and under the HAECs, and the SPs were stably located after 48 h of incubation. The time-dependent and localized NO concentration on surrounding area of cells in response to bradykinin stimulation will be detected distinctly. The fluorescence intensity in 3 μm circle area containing one SP in CLSM images was measured, and then the NO concentration was estimated from the calibration curve (see Figure S4a in the Supporting Information). When bradykinin was added to the culture medium, the NO concentration at the apical membrane (on the cells) rapidly increased to about 110% within 5 min, and was subsequently stable over 2 h (Figure 2c). In contrast, the NO concentration at the basal membrane (under the cells) also rapidly increased to over 140%, and reached a stable value after 40 min (Figure 2d). The SPs under the HAECs showed a clear difference of CLSM images before and after bradykinin stimulation (see Figure S4b–e in the Supporting Information). These results suggest that NO production from the basal membrane is higher than that of the apical membrane. To evaluate the 3D structural effect of the cellular alignment on localized NO production, the NO concentration at the apical and basal membranes of the HAECs in monolayers or bilayers after 48 h of incubation was analyzed by the SPs (Figure 2e). The NO concentrations at the basal membrane of the HAECs in the monolayer and bilayer were 4.5-fold and twofold higher, respectively, than those on the HAEC surfaces, suggesting that the NO molecule was more readily produced at the basal membrane than at the apical membrane independent of 3D layered structure. Interestingly, similar to that shown in Figure S3, the bilayer structure showed higher local NO concentrations at both the apical and basal membranes than did a monolayer of HAECs. The localized NO concentration on the AoSMCs analyzed by the SPs was less than 10 nM, which is almost the detection limit of the SPs. The reason for this difference in NO production at the basal

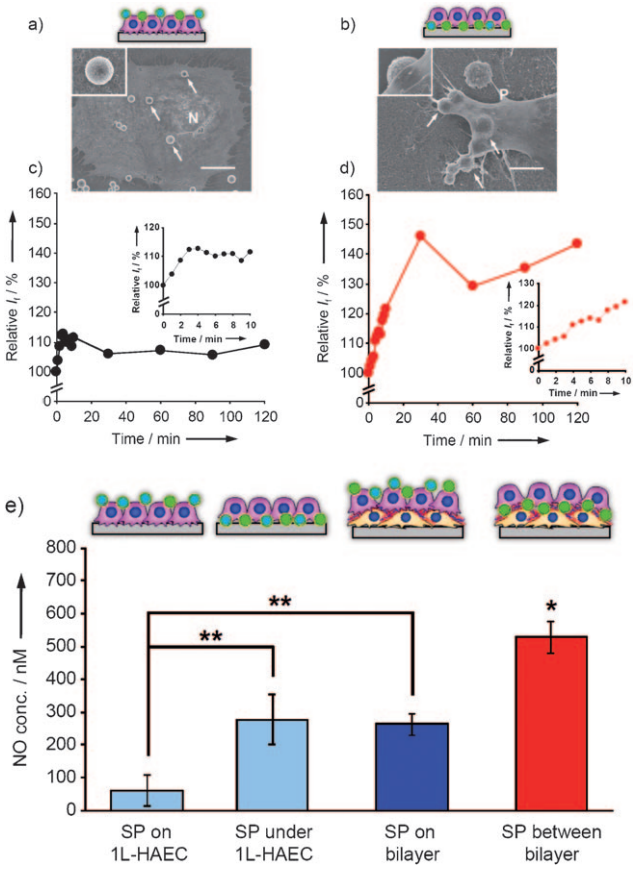

Figure 2. a,b) SEM images of SPs on (a) and under (b) 1L-HAEC. N, P, and the arrows indicate the nuclei, pseudopodia, and SPs, respectively. The insets show magnified SEM images of each SP. c,d) Relative fluorescence intensity changes of SPs on (c) and under (d) 1 L-HAEC at 37 °C for 2 h after the addition of 2.5 μM bradykinin. The averaged fluorescence intensity of the SPs was measured from the CLSM images ($n = 3$, over 20 SPs per image). The relative percentage was calculated from a comparison with the fluorescence intensity at $t = 0$ min (control, 100%). The insets show the relative fluorescence intensities within 10 min. e) Localized NO diffusion analyses in relation to 3D structural effects. The localized NO concentrations were analyzed by SPs on and under the HAECs in monolayers and bilayers after 48 h of incubation. The averaged fluorescence intensity of the SPs was measured from CLSM images ($n = 3$, over 20 SPs per image), and the NO concentration was estimated from the calibration curve of Figure S4a in the Supporting Information. The asterisks denote a statistically significant difference using a two-sample t test (**: $p < 0.05$; *: $p < 0.01$) for each comparison or comparison with all other samples. I_f = fluorescence intensity.

and apical sides would be related to the localization of NOS in the HAECs. Ortiz et al. recently reported that endothelial NOS (eNOS) was highly localized around the middle and basal sides of the endothelial cells in the rat ascending limb.[9b] Accordingly, the amount of NO production at the basal membrane was higher than that at the apical membrane. The difference of localized NO concentration around the endothelial cells could be clarified for the first time by using the NO sensor particles.

Finally, we demonstrated a quantitative 3D analysis of NO diffusion from the uppermost 1L-HAECs to the underlying 4L-AoSMCs in 5L-artery models using the SPs. The SPs were allocated into each layer as shown in Figure 1. Figure 3a shows reconstructed 3D CLSM images of the 5L constructs after 48 h of culture, where green and blue represent the SPs and nuclei, respectively. The averaged local NO concentrations in each layer were quantified from the cross-sectional image (Figure 3b) and summarized in Figure 3c. The NO concentrations in first (HAEC) and second (AoSMC) layers were about 530–550 nM, and then gradually decreased with increasing layer number. The NO concentration reached about 50% (290 nM) in the fifth layer (32 μm in depth). Furthermore, the distance of NO diffusion from the top HAEC layer to the underlying AoSMC layers was estimated at approximately 60 μm from the equation in Figure S5 (see the Supporting Information), which shows the correlation

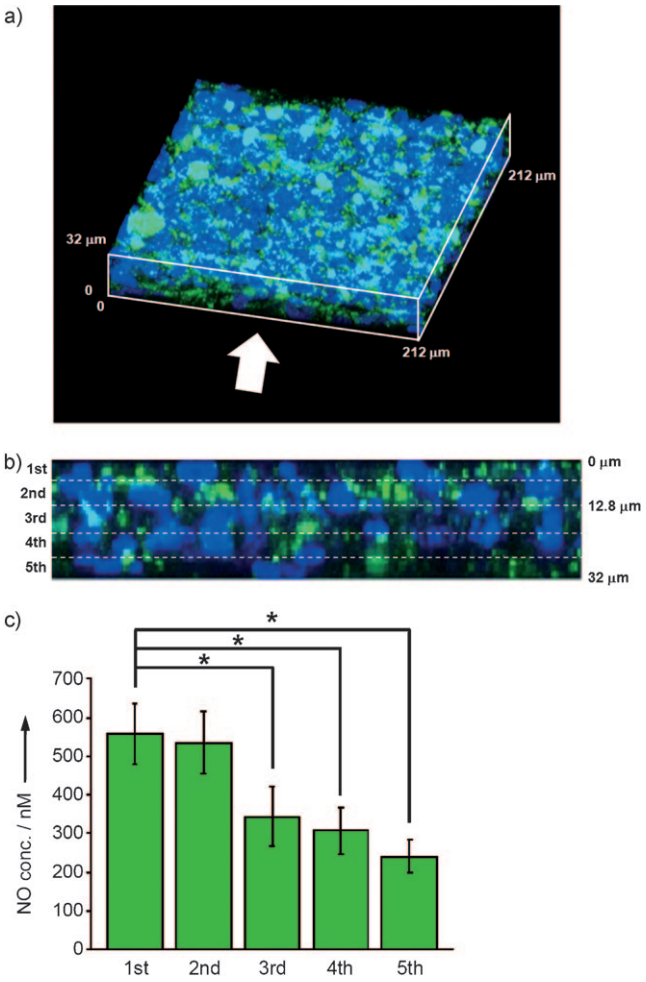

Figure 3. a) Reconstructed 3D CLSM image of the 5L-artery model containing SPs (green) in each layer after 48 h of incubation. The 1st layer is HAECs, and the 2nd to 5th layers are AoSMCs. The nuclei (blue) were labeled with 4′,6-diamidino-2-phenylindole dihydrochloride (DAPI). The image area is 212.1×212.1 μm^2, and the height is 32.0 μm. b) Cross-sectional CLSM image of (a) in the direction of the white arrow. The dashed lines indicate brief interfaces of each layer. c) Localized NO concentrations in each cellular layer were analyzed by SPs. The fluorescence intensities of the SPs were measured from each layer (6.4×212.1 μm^2) in (b) ($n = 3$, over 20 SPs per image). The asterisks denote a statistically significant difference using a two-sample t test (*: $p < 0.01$) for each comparison.

between the NO concentration and the distance from the HAECs. Although this value is slightly lower than the reported in vivo NO diffusion distance of approximately 100 μm,[5b,c] the obtained value is reasonable because it is known that about 37% of the produced NO is consumed in chemical reactions in the artery walls.[5c] These results suggest that this technique will be a useful method for in vitro artery assays to replace in vivo animal experiments.

In summary, we demonstrated the in vitro 3D analysis of NO diffusion in an artery wall by the construction of 3D artery layered models including SPs. Our method does not require special instruments or techniques and is convenient and effective for drug screening, and thus it has possibility to be a solution of general animal experiments. Recently, the development of in vitro 3D bioassay systems of tissue responses such as the lung,[10a] tumors,[10b] and neurons[10c] have been reported, and the in vitro bioassay of 3D tissue models are currently key issues in the biomaterial and biotechnology fields. To the best of our knowledge, this is the first example of 3D assay of NO diffusion using an engineered 3D artery model. Further detailed experiments under blood and blood-flow conditions to reflect a natural artery condition more accurately are now in progress, taking into account a comparison with mathematical models of NO diffusion, because NO diffusion in this study was interpreted as a simplistic diffusion. Since this sensor particle technology can be applied to the other fluorescent indicator dyes such as Fura-4F for calcium ion and seminaphthorhodafluor-1 (SNARF-1) for pH changes (see Figure S6 in the Supporting Information), its versatile applications for analyzing extracellular diffusion of various signal molecules in 3D tissue models can be expected.

Experimental Section

Preparation of NO sensor particles: A 5 mg mL^{-1} CT solution was vigorously stirred with two molar equivalents of HOBt in deionized water at ambient temperature until the solution turned clear. The resultant solution was diluted to 1 mg mL^{-1} and the solution pH was adjusted to around 7 by adding 1M NaOH. Mesoporous silica particles of 1.6 μm diameter were immersed alternately into a 1 mg mL^{-1} CT solution ($M_w = 6.5 \times 10^5$) containing HOBt (pH 6.8, 0.5M NaCl) and a 1 mg mL^{-1} DS solution ($M_w = 5.0 \times 10^5$, pH 6.6, 0.5M NaCl) for 15 min. Collection of the particles after each immersion was performed by centrifugation at 2000 rpm for 3 min. The immersion was repeated five times, and the CT-DS LbL films were prepared on the silica particles. The mean thickness of the CT–DS films was estimated to be approximately 40 nm by quartz crystal microbalance (QCM) measurements[8a]

Fabrication of 3D artery models with SPs: Human AoSMCs (CAMBREX, USA) and HAECs (CAMBREX, USA) at passages 5 to 7 were used in the present study. The AoSMCs were cultured in smooth-muscle basal medium (SmBM; CAMBREX, USA) containing human epidermal growth factor (hEGF), human fibroblast factor basic (hFGF-B), GA-1000, fetal bovine serum (FBS), and insulin. The HAECs were cultured in endothelial basal medium-2 (EBM-2; CAMBREX, USA) containing hFGF-B, vascular endothelial growth factor (VEGF), R3-IGF-1 (IGF-1 = insulin-like growth factor-1), ascorbic acid, FBS, hEGF, and GA-1000. For the culture of the multilayers, Dulbecco's modified eagle medium (DMEM; Wako, Pure Chemical Inc., Japan) with 10% FBS was used as a culture medium. A cell desk LF (7.07 cm^2; Smitomo Bakelite Co, Ltd., Japan) or cover slip was used as the substrate. The substrate was immersed into a 50 mM Tris-HCl buffer solution (pH 7.4) of FN (0.2 mg mL^{-1}) for 15 min, and AoSMCs (4×10^4 cell cm^{-2}) were seeded onto the substrate and cultured for 24 h at 37°C. The monolayered cells were rinsed with Tris buffer, and then alternately immersed into the FN solution and 50 mM Tris-HCl buffer solution (pH 7.4) of G (0.2 mg mL^{-1}) for 1 min per solution. The sample was taken, and rinsed with Tris buffer. After the seven-step assembly of FN and G, the SP solution at 0.2 mg mL^{-1} in DMEM was dropped onto the cell surface, and incubated for 10 min to allow the adsorption of the SPs onto the FN-G films on the cell surfaces. The substrate was then gently washed with Tris buffer, and AoSMCs (4×10^4 cell cm^{-2}) as the second layer were seeded and incubated for 24 h at 37°C. After repeating these steps to generate four-layered AoSMCs with SPs in each layer, HAECs (6×10^4 cell cm^{-2}) were seeded and incubated for 24 h to fabricate the uppermost layer. For SEM observation, the 1L-HAECs with SPs were immersed into a 10% formalin aqueous solution for 10 min, and then subsequently immersed into a graded series of ethanol for dehydration, followed by *tert*-butyl alcohol for 2 h. They were freeze-dried and coated with platinum. SEM observations were performed using a JSM-6701F electron microscope (JOEL Co. Ltd., Japan).

Additional methods: Detailed methods regarding stability of the SPs, HRP assay, calibration curve, and development of calcium and pH sensor particles are available in the Supporting Information.

Received: December 27, 2010
Revised: March 2, 2011
Published online: June 30, 2011

Keywords: biosensors · cell adhesion · layered compounds · nitrogen oxides · thin films

[1] B. C. Isenberg, J. Y. Wong, *Mater. Today* **2006**, *9*, 54–60.
[2] a) A. Kadi, N. de Isla, P. Lacolley, J. F. Stoltz, P. Menu, *Clin. Hemorheol. Microcirc.* **2007**, *37*, 131–140; b) Y. S. J. Li, J. H. Haga, S. Chien, *J. Biomech. Eng.* **2005**, *38*, 1949–1971.
[3] J. R. Lancaster, Jr., *Nitric Oxide* **1997**, *1*, 18–30.
[4] a) L. J. Ignarro, G. M. Buga, K. S. Wood, R. E. Byrns, G. Chaudhuri, *Proc. Natl. Acad. Sci. USA* **1987**, *84*, 9265–9269; b) E. Clementi, G. C. Brown, M. Feelisch, S. Moncada, *Proc. Natl. Acad. Sci. USA* **1998**, *95*, 7631–7636; c) J. B. Mannick, A. Hausladen, L. Liu, D. T. Hess, M. Zeng, Q. X. Miao, L. S. Kane, A. J. Gow, J. S. Stamler, *Science* **1999**, *284*, 651–654.
[5] a) W. K. Alderton, C. E. Cooper, R. G. Knowles, *Biochem. J.* **2001**, *357*, 593–615; b) T. Malinski, Z. Taha, *Nature* **1992**, *358*, 676–678; c) T. Malinski, Z. Taha, S. Grunfeld, *Biochem. Biophys. Res. Commun.* **1993**, *193*, 1076–1082.
[6] a) H. Kojima, N. Nakatsubo, K. Kikuchi, S. Kawahara, Y. Kirino, H. Nagoshi, Y, Hirata, T. Nagano, *Anal. Chem.* **1998**, *70*, 2446–2453; b) H. Kojima, Y. Urano, K. Kikuchi, T. Higuchi, Y. Hirata, T. Nagano, *Angew. Chem.* **1999**, *111*, 3419–3422; *Angew. Chem. Int. Ed.* **1999**, *38*, 3209–3212.
[7] a) N. Nakatsubo, H. Kojima, K. Kikuchi, H. Nagoshi, Y. Hirata, D. Maeda, Y. Imai, T. Irimura, T. Nagano, *FEBS Lett.* **1998**, *427*, 263–266; b) S. Amemori, M. Matsusaki, M. Akashi, *Chem. Lett.* **2010**, *39*, 42–43.
[8] a) M. Matsusaki, K. Kadowaki, Y. Nakahara, M. Akashi, *Angew. Chem.* **2007**, *119*, 4773–4776; *Angew. Chem. Int. Ed.* **2007**, *46*, 4689–4692; b) K. Kadowaki, M. Matsusaki, M. Akashi, *Langmuir* **2010**, *26*, 5670–5678; c) K. Kadowaki, M. Matsusaki, M. Akashi, *Biochem. Biophys. Res. Commun.* **2010**, *402*, 153–157; d) M. Matsusaki, K. Kadowaki, E. Adachi, T. Sakura, U. Yokoyama, Y. Ishikawa, M. Akashi, *J. Biomater. Sci. Polym. Ed.* **2011**, DOI: 10.1163/092050610X541953.

[9] a) K. Kikuchi, T. Nagano, M. Hirobe, *Biol. Pharm. Bull.* **1996**, *19*, 649 – 651; b) P. A. Ortiz, N. J. Hong, J. L. Garvin, *Am. J. Physiol. Renal. Physiol.* **2004**, *287*, F274 – F280.
[10] a) D. Huh, B. D. Matthews, A. Mammoto, M. Montoya-Zavala, H. Y. Hsin, D. E. Ingber, *Science* **2010**, *328*, 1662 – 1668; b) C. Fischbach, R. Chen, T. Matsumoto, T. Schmelzle, J. S. Brugge, P. J. Polverini, D. J. Mooney, *Nat. Methods* **2007**, *4*, 855 – 860; c) S. Pautot, C. Wyart, E. Y. Isacoff, *Nat. Methods* **2008**, *5*, 735 – 740.

